Inorg. Chem. **2000,** *39,* 5014−5021

Influence of H_2S and Thiols on the Binding of Alkenes and Alkynes to ReS_4^-: The Spectator Sulfido Effect

Joel A. Dopke, Scott R. Wilson, and Thomas B. Rauchfuss*

Department of Chemistry, University of Illinois at Urbana-Champaign, Urbana, Illinois 61801

Received February 15, 2000

The three-component reaction of ReS_4^- (**1**), H_2S, and unsaturated substrates (un = alkene, alkyne) affords the Re^V derivatives $Re(S)(S_2un)(SH)_2^-$. These adducts arise via the addition of H_2S to intermediate dithiolates $ReS_2(S_2C_2R_4)^-$ and dithiolenes $ReS_2(S_2C_2R_2)^-$. The species $\{ReS[S_2C_2(tms)_2](SH)_2\}^-$, $[ReS(S_2C_7H_{10})(SH)_2]^-$ (**3**), and $[ReS(S_2C_2H_4)(SH)_2]^-$ are prepared according to this route. Similarly, the selenolate−thiolate complex $[ReS(S_2C_7H_{10})(SeH)(SH)]^-$ (**5**) is produced by the reaction of $[ReS_2(S_2C_7H_{10})]^-$ with H_2Se. The corresponding reactions using benzenethiol in place of H_2S afford the more thermally robust adducts $\{ReS[S_2C_2(tms)_2](SH)(SPh)\}^-$, $[ReS(S_2C_7H_{10})(SH)(SPh)]^-$ (**7**), and $[ReS(S_2C_2H_4)(SH)(SPh)]^-$. Norbornanedithiolato compounds **3**, **5**, and **7** are obtained as pairs of isomers that differ in terms of the relative orientation of the norbornane bridgehead relative to the Re═S unit. The reaction of $[ReS(S_2C_7H_{10})(SD)_2]^-$ (**3**-d_2) with H_2S to give **3** is proposed to proceed via elimination of D_2S and subsequent addition of H_2S. Variable-temperature ^1H NMR measurements on the equilibrium of $[ReS(S_2C_6H_{12})(SPh)(SH)]^-$ with **1**, 1-hexene, and PhSH gave the following results: $\Delta H = -7\ (\pm 1)\ kJ{\cdot}mol^{-1}$; $\Delta S = 23\ (\pm 4)\ J{\cdot}mol^{-1}{\cdot}K^{-1}$. Solutions of ethanedithiol and **1** react with $C_2(tms)_2$ and C_2H_4 to give $\{ReS[S_2C_2(tms)_2](S_2C_2H_4)\}^-$ and $[ReS(S_2C_2H_4)_2]^-$, respectively, concomitant with loss of H_2S. The pathway for the ethanedithiol reaction is examined using 2-mercaptoethanol, affording $\{ReS[S_2C_2(tms)_2](SC_2H_4OH)\}^-$, which does not cyclize. Treatment of a solution of diphenylbutadiyne and **1** with PhSH gives two isomers of the dithiolene $\{ReS(SH)(SPh)[S_2C_2Ph(C_2Ph)]\}^-$. The corresponding reaction of ethanedithiol, diphenylbutadiyne, and **1** affords the 1,4-diphenylbutadiene-1,2,3,4-tetrathiolate complex $\{[ReS(S_2C_2H_4)]_2(S_4C_4Ph_2)\}^{2-}$.

Introduction

Hydrodesulfurization (HDS) is a large-scale industrial process utilized to remove sulfur from petroleum via hydrogenolysis (eq 1). HDS is the subject of intense research because of its

$$R{-}S{-}R + 2\,H_2 \xrightarrow{MS_n\ \text{catalyst}} 2\,RH + H_2S \qquad (1)$$

environmental implications.[1,2] This process is catalyzed by metal sulfides, typically MoS_x/CoS_y, but the sulfides of rhenium, ruthenium, and other metals are even more active.[3] Much of this HDS-directed research is directed toward the development of homogeneous catalysts.[4,5] Solution-phase work also provides a wealth of mechanistic and structural insights.[6]

Both organometallic and inorganic systems have been investigated as homogeneous models for HDS. For example, the organometallic species Cp^*_2TiS,[7−9] $(PR_3)_6Rh_2S_2^{2+}$,[10] and $Cp_2Mo_2S_4$[11] have been found to be capable of activating H_2. Extensive research on the tetrathiometalate anions MS_4^{n-} (M = V, Nb, Ta, $n = 3$; M = Mo, W, $n = 2$; M = Re, $n = 1$)[12,13] has provided fundamental insights into the reactivity of the M═S group[14] without the complicating effects of ancillary organic ligands. Generally, the M═S group is more reactive than M═O due to the weaker π-donor ability of S^{2-}.[14] For similar reasons, thiometalates are better electron acceptors than the corresponding oxometalates,[15] and the $M(S)_2{-}M(\eta^2\text{-}S_2)$ equilibrium is more energetically accessible than $M(O)_2{-}M(\eta^2\text{-}O_2)$.[16]

Because molybdenum sulfides are the principal HDS catalysts, the reactivity of thiomolybdates such as MoS_4^{2-} been of particular interest. Coucouvanis and Stiefel have amply demonstrated the ability of thiomolybdates to bind unsaturated substrates such as activated alkynes, sulfur dioxide, and carbon disulfide.[13] Thiomolybdates, however, display little or no affinity for alkenes, dihydrogen, or the organosulfur species found in petroleum. In contrast, ReS_4^- (**1**), which is isoelectronic and

---

(1) McCoy, M. *Chem. Eng. News* **1999**, 17−25.
(2) Upson, L. L.; Schnaith, M. W. *Oil Gas J.* **1997**, 47−51.
(3) Chianelli, R. R.; Pecoraro, T. A.; Halbert, T. R.; Pan, W. H.; Stiefel, E. I. *J. Catal.* **1984**, *86*, 226−230.
(4) Curtis, M. D. *ACS Symp. Ser.* **1996**, *No. 653*, 154−175.
(5) Bianchini, C.; Meli, A. *Acc. Chem. Res.* **1998**, *31*, 109−116.
(6) Angelici, R. J. In *Encyclopedia of Inorganic Chemistry*; King, R. B., Ed.; John Wiley: New York, 1994; pp 1433−1443.
(7) Sweeney, Z. K.; Polse, J. L.; Andersen, R. A.; Bergman, R. G.; Kubinec, M. G. *J. Am. Chem. Soc.* **1997**, *119*, 4543−4544.
(8) Sweeney, Z. K.; Polse, J. L.; Andersen, R. A.; Bergman, R. G. *J. Am. Chem. Soc.* **1998**, *120*, 7825−7834.
(9) Sweeney, Z. K.; Polse, J. L.; Andersen, R. A.; Bergman, R. G. *Organometallics* **1999**, *18*, 5502−5510.
(10) Bianchini, C.; Mealli, C.; Meli, A.; Sabat, M. *Inorg. Chem.* **1986**, *25*, 4617−4618.
(11) Rakowski DuBois, M.; Jagirdar, B.; Noll, B.; Dietz, S. *ACS Symp. Ser.* **1996**, *No. 653*, 269−281.
(12) Müller, A.; Diemann, E.; Jostes, R.; Bögge, H. *Angew. Chem., Int. Ed. Engl.* **1981**, *20*, 934.
(13) Coucouvanis, D. *Adv. Inorg. Chem.* **1998**, *45*, 1−73. Stiefel, E. I. *ACS Symp. Ser.* **1996**, *No. 653*, 2−38.
(14) Parkin, G. *Prog. Inorg. Chem.* **1998**, *47*, 1−166.
(15) Goodman, J. T.; Rauchfuss, T. B. *J. Am. Chem. Soc.* **1999**, *121*, 5017−5022.
(16) Schroeder, D.; Kretzschmar, I.; Schwarz, H.; Rue, C.; Armentrout, P. B. *Inorg. Chem.* **1999**, *38*, 3474−3480.

10.1021/ic0001661 CCC: $19.00

Scheme 1[a]

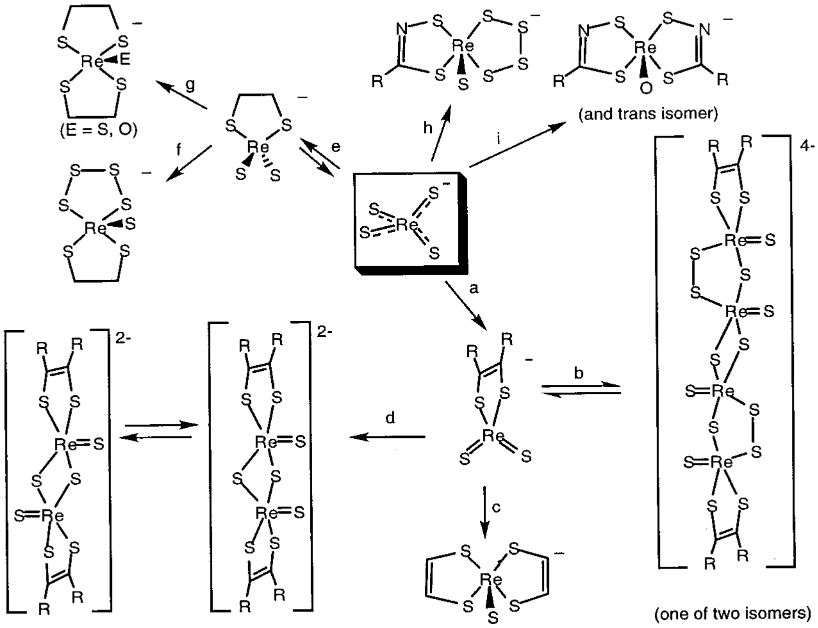

[a] Key: a, C_2R_2; b, ReS_4^-; c, C_2R_2 + S; d, 25 °C; e, C_2R_4; f, S_8; g, C_2R_4 + S or NMO; h, RCN + S_8; i, CF_3CN + NMO.

isostructural with MoS_4^{2-}, reacts with alkenes and alkynes (un) to produce the tetrahedral d^2 adducts $ReS_2(S_2un)^-$ (Scheme 1).[15,17−19]

The influence of H_2S on the affinity of metal sulfides for organic substrates is relevant to HDS because H_2S and such organic substrates coexist under catalytic conditions, with H_2S being a coproduct of C−S bond hydrogenolysis. H_2S has been shown to inhibit HDS[20−24] and strongly poisons other kinds of catalysis. Interestingly, the effect of H_2S on toluene hydrogenation by Co−MoS catalysts follows complex kinetics with relatively little inhibition at low P_{H_2S}.[25] The interaction of H_2S and metal sulfides is also relevant to the addition of HR to E=M=O moieties to give Mo(EH)(O)(R), which has been invoked in the catalytic mechanism of xanthine oxidase.[26−29] In the present paper, we describe the surprising influence of H_2S and thiol reagents on the affinity of **1** for unsaturated substrates.

Results and Discussion

Scheme 2

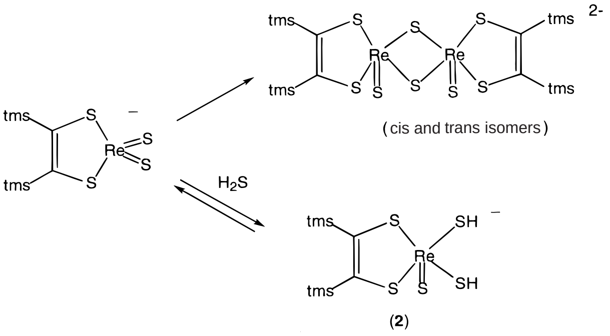

Adducts with H_2S. Monomeric $ReS_2[S_2C_2(tms)_2]^-$, generated in situ by treatment of an CH_3CN solution of **1** with bis(trimethylsilyl)acetylene, reacts rapidly with H_2S to give the red-brown adduct **2**. ^1H NMR analysis indicates that **2** is symmetrical with equivalent S*H* groups (*δ* 5.98). The assignment of **2** as $\{ReS[S_2C_2(tms)_2](SH)_2\}^-$ is supported by an electrospray ionization mass spectrometry (ESI-MS) analysis showing a parent mass envelope at *m*/*z* = 519.1. Solutions of **2** degrade over the course of several hours to give $\{Re(\mu\text{-}S)S[S_2C_2(tms)_2]\}_2^{2-}$ (Scheme 2), which was previously shown to arise via the dimerization of the monodithiolene $ReS_2[S_2C_2(tms)_2]^-$.[19] Attempts to convert the dimer $\{Re(\mu\text{-}S)S[S_2C_2(tms)_2]\}_2^{2-}$ to **2** under 1 atm of H_2S were unsuccessful.

We also examined the interaction of H_2S with the alkanedithiol*a*tes $[ReS_2(S_2C_2R_4)]^-$, which, in contrast to the dithiol*e*nes $[ReS_2(S_2C_2R_2)]^-$, show no tendency to dimerize. The norbornene adduct of **1** adds H_2S to produce the adduct $[ReS(S_2C_7H_{10})(SH)_2]^-$ (**3**), as supported by ^1H NMR spectroscopy and by elemental and mass spectral analyses. Compound **3** exists as a pair of isomers with δ_{SH} = 6.07 and 6.08. Since the addition of norbornene to ReS_4^- is exclusively exo,[15] the isomerism is assumed to arise from the relative orientation of the Re=S unit relative to the apical methylene of the norbornanedithiolate. MeCN solutions of the isomers of **3** do not convert to a single isomer upon the addition of 1,8-bis(dimethylamino)naphthalene (Proton Sponge), $[ReS_2(S_2C_7H_{10})]^-$, or H_2S. Solutions of **3** sealed under vacuum cleanly revert to $[ReS_2(S_2C_7H_{10})]^-$ and

---

(17) Goodman, J. T.; Inomata, S.; Rauchfuss, T. B. *J. Am. Chem. Soc.* **1996**, *118*, 11674−11676.
(18) Goodman, J. T.; Rauchfuss, T. B. *Angew. Chem., Int. Ed. Engl.* **1997**, *36*, 2083−2084.
(19) Goodman, J. T.; Rauchfuss, T. B. *Inorg. Chem.* **1998**, *37*, 5040−5041.
(20) Nag, N. K.; Fraenkel, D.; Moulijn, J. A.; Gates, B. C. *J. Catal.* **1980**, *66*, 162−170.
(21) Bussell, M. E.; Somorjai, G. A. *J. Catal.* **1987**, *106*, 93−104.
(22) Ramachandran, R.; Massoth, F. E. *Can. J. Chem. Eng.* **1982**, *60*, 17−22.
(23) Burch, R.; Collins, A. *Appl. Catal.* **1985**, *18*, 373−387.
(24) Dianis, W. P. *Appl. Catal.* **1987**, *30*, 99−121.
(25) Graf, D. D.; Mann, K. R. *Inorg. Chem.* **1997**, *36*, 141−149.
(26) Coucouvanis, D.; Toupadakis, A.; Lane, J. D.; Koo, S. M.; Kim, C. G.; Hadjikyriacou, A. *J. Am. Chem. Soc.* **1991**, *113*, 5271−5282.
(27) Bray, M. R.; Deeth, R. J. *J. Chem. Soc., Dalton Trans.* **1997**, 1267−1268.
(28) Ilich, P.; Hille, R. *J. Phys. Chem. B* **1999**, *103*, 5406−5412.
(29) Huber, R.; Hof, P.; Duarte, R. O.; Moura, J. J. G.; Moura, I.; Liu, M.-Y.; LeGall, J.; Hille, R.; Archer, M.; Romão, M. J. *Proc. Natl. Acad. Sci. U.S.A.* **1996**, *93*, 8846−8851.

H_2S over the course of several days. Throughout this conversion, the ratio of the two isomers does not change.

Treatment of a solution of $[ReS_2(S_2C_7H_{10})]^-$ with H_2Se yields a spectroscopically pure derivative assigned as $[ReS(S_2C_7H_{10})(SH)(SeH)]^-$ (**5**). Two ^1H NMR signals are observed in both the S*H* (δ 6.71, 6.67) and the more shielded Se*H* (δ 2.51, 2.49) regions. The low-field signals are assigned to S*H*, while the pair of high-field signals are assigned to Se*H*. It is typical for RSe*H* signals to occur at ca. 5 ppm higher field than the corresponding RS*H* signals.[30] While $^1J_{SeH}$ is obscured by surrounding signals, the $^3J_{SeH}$ coupling to terminal $-SH$ protons is observed to be 13.5 Hz. The observation of two Se*H* and two S*H* signals is consistent with the formation of two diastereomers (eq 2).

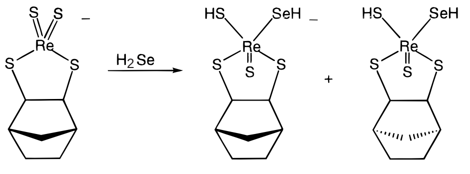

(2)

diastereomers of **5**

The H−D exchange properties of $[ReS(S_2C_7H_{10})(SD)_2]^-$ (**3**-d_2) were next examined. H_2S-saturated CD_3CN solutions of **3**-d_2 undergo exchange of terminal ReS*D*; the slowness of the H−D exchange process argues against simple proton transfer. Instead, we propose that H−D exchange proceeds via dissociation of D_2S from **3**-d_2 to form $[ReS_2(S_2C_7H_{10})]^-$, which subsequently adds H_2S to re-form **3** (eq 3).

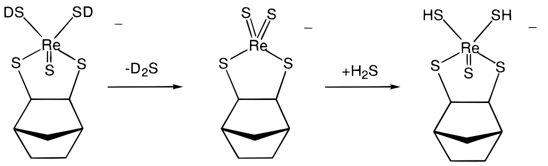

(3)

5-d_2 (one of two diastereomers)

5 (one of two diastereomers)

The three-component reaction of **1**, H_2S, and ethylene was characterized *in situ* by ^1H NMR spectroscopy. Under typical conditions, a 61% conversion of **1** to $[ReS(S_2C_2H_4)(SH)_2]^-$ (**4**) was realized, as judged by comparison of the integrated intensities of the Ph_4P^+ cation and the AA′BB′ multiplet for the $S_2C_2H_4$ unit. At low temperatures, the ethylene adduct $[ReS_2(S_2C_2H_4)]^-$ is readily observed in addition to **4**. Upon removal of H_2S and C_2H_4, the color of the solution changes from red-brown (characteristic of **4**) to violet, characteristic of **1**. The reaction of **1**, H_2S, and C_2H_4 is fully reversible.

Adducts Prepared from PhSH. Adducts derived from PhSH proved to be more readily isolable than those derived from H_2S. Additions of the unsaturated substrates to solutions of **1** and a slight excess of the thiol produced the desired adducts. In this way, the brown Ph_4P^+ salt of $\{ReS[S_2C_2(tms)_2](SH)(SPh)\}^-$ (**6**) was prepared from $C_2(tms)_2$, **1**, and PhSH. Similarly, the norbornanedithiolate $[ReS_2(S_2C_7H_{10})]^-$ adds PhSH to give $[ReS(S_2C_7H_{10})(SH)(SPh)]^-$ (**7**). The ^1H NMR data for **7** are consistent with two independent spin systems, one with $\delta_{SH} =$ 5.91 and the other with $\delta_{SH} = 5.87$. As in the case of **3**, isomerism is attributed to the orientation of the apical methylene relative to the axial Re═S.

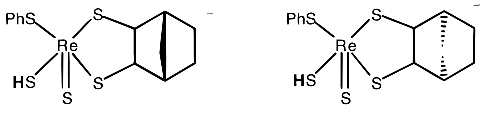

Diastereomers of **7**

The reaction of **1**, C_2H_4, and PhSH afforded the adduct $[ReS(S_2C_2H_4)(SH)(SPh)]^-$ (**8**). In contrast to $[ReS(S_2C_2H_4)(SH)_2]^-$, **8** is easily isolable. While the structure of **8** is unambiguously defined (Figure 1), refinement was limited because of a twinning problem. Anion **8** adopts the expected square pyramidal geometry with an axial sulfido ligand. The rhenium atom lies 0.748 Å above the best plane through the four basal sulfur atoms (mean deviation from planarity: 0.023 Å). The M−S*H* was not located crystallographically, but the Re−S(H) bond distance of 2.353 Å is consistent with a single bond.

As in the case of substituted alkenes,[15] 1-hexene binds to **1** more weakly than does C_2H_4. Consequently, this substrate provides a convenient test of the ability of thiols to stabilize alkene binding. The adduct $[ReS(S_2C_6H_{12})(SPh)(SH)]^-$ (**9**) could in fact be observed, although relatively high concentrations of alkene and thiol were required. The K_{eq}(294 K) value for the reaction of Ph_4P[**1**] with 1-hexene and PhSH was determined to be 402 M^{-2} by ^1H NMR spectroscopy. The ^1H NMR spectrum of **9** is complex in the C*H* region, although four well-resolved Re−S*H* singlets (δ 6.54, 6.43, 6.39, 6.38) are observed. These correspond to the four diastereomers arising from the relative orientations of the butyl substituent, the Re−SR group (R = Ph), and the Re═S unit:

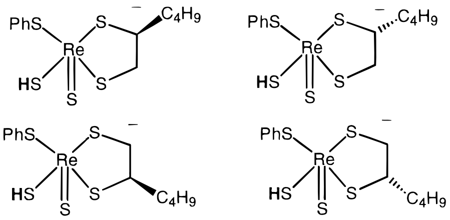

Diastereomers of **9**

In the absence of PhSH, there is no evidence for the interaction of **1** and 1-hexene at room temperature. The upper bound for the binding of **1** to $[ReS_2(S_2C_6H_{12})]^-$ (298 K) is estimated as 0.84 M^{-1} with the assumption of 5% conversion of **1** to $[ReS_2(S_2C_6H_{12})]^-$. It follows that the equilibrium constant for the binding of thiol by the Re^V−alkene adduct is >478 M^{-1}.

We studied the temperature dependence of the formation of **9** from **1**, 1-hexene, and benzenethiol (Scheme 3). At room temperature the equilibrium constant (K_{eq}) is 402 M^{-2} (Table 1). The temperature dependence of this binding indicates ΔH and ΔS of −7 (±1) kJ·mol^{-1} and 23 (± 4) J·mol^{-1}·K^{-1}, respectively (Figure 2).

Reactions Involving Dithiols. The use of dithiols extends the newly developed reactivity of $[ReS_2(S_2C_2R_n)]^-$ with RSH reagents. A solution of the dithiolene $\{ReS_2[S_2C_2(tms)_2]\}^-$ and ethanedithiol evolves H_2S to afford a unique example of a mixed alk*a*nedithiolate−alk*e*nedithiolate, $\{ReS[S_2C_2(tms)_2](S_2C_2H_4)\}^-$ (**10**). A crystallographic characterization of **10** confirmed the square pyramidal coordination environment about the rhenium with two different chelating dithio ligands (Figure 3). The Re−S(dithiolene) bonds are shorter than the Re−S(dithiolate) bonds by only 0.02 Å. The rhenium−sulfur distances for the dithiolate and dithiolene ligands fall within the

---

(30) Amarasekera, J.; Houser, E. J.; Rauchfuss, T. B.; Wilson, S. R. *Inorg. Chem.* **1992**, *31*, 1614−1620.

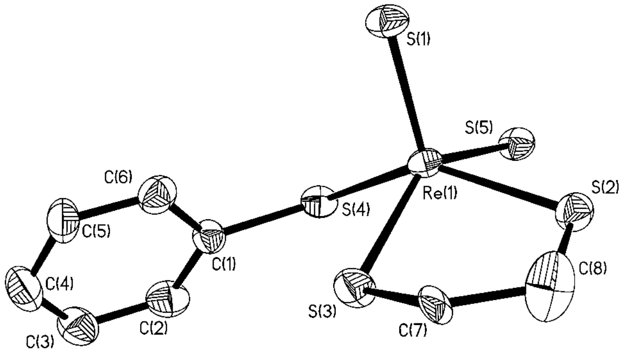

Figure 1. Structure of the anion $[ReS(S_2C_2H_4)(SH)(SPh)]^-$ (**8**) with thermal ellipsoids drawn at the 35% probability level. The more highly populated C(7) position in the disordered ethanedithiolate is shown, and hydrogen atoms are omitted for clarity.

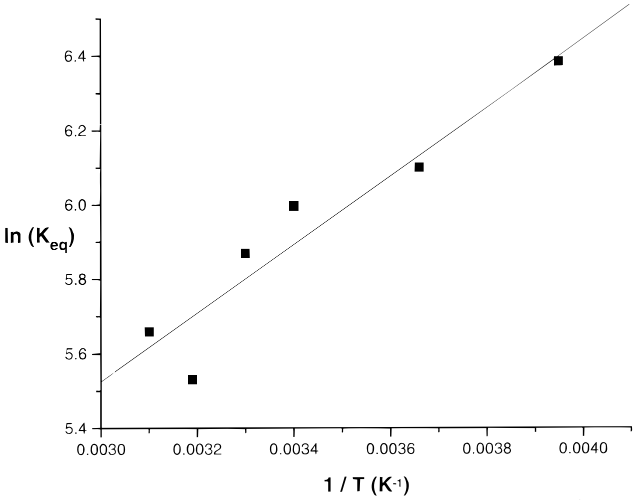

Figure 2. Van't Hoff plot for the equilibrium of $Ph_4P[\mathbf{9}]$ with $Ph_4P[\mathbf{1}]$, 1-hexene, and PhSH.

Scheme 3

$$ReS_4^- + CH_2{=}CHC_4H_9 \rightleftharpoons S_2Re(S_2C_6H_{12})^- \quad K_1$$

$$S_2Re(S_2C_6H_{12})^- + PhSH \rightleftharpoons ReS(S_2C_6H_{12})(SH)(SPh)^- \quad K_2$$

$$ReS_4^- + CH_2{=}CHC_4H_9 + PhSH \rightleftharpoons ReS(SH)(SPh)(S_2C_6H_{12})^- \quad K_{12}$$

$$K_{12} = [ReS(S_2C_6H_{12})(SH)(SPh)^-]/[ReS_4^-][CH_2{=}CHC_4H_9][PhSH]$$

Table 1. Observed Concentrations for the Variable-Temperature ^1H NMR Study of the Equilibrium of ReS_4^- (**1**), 1-Hexene, and PhSH with $[ReS(S_2C_6H_{12})(SPh)(SH)^-]$ (**9**) in CD_3CN

	concn (mM)				
T (°C)	**9**	1-hexene	PhSH	ReS_4^-	K_{eq} (M^{-2})
−20	2.38	69.8	91.6	0.627	592
0	2.19	67.9	89.2	0.811	446
21	2.07	63.5	86.3	0.937	402
30	1.98	62.6	86.7	1.027	354
40	1.79	65.0	90.3	1.210	252
50	1.93	67.9	92.0	1.075	287

observed ranges for bis(dithiolene) and bis(dithiolate) rhenium complexes. The rhenium atom lies 0.613 Å above the best plane through the four basal sulfur atoms (mean deviation from planarity: 0.001 Å). The only previously reported example of a mixed dithiolene−dithiolate complex is $Tc_2(\mu\text{-}S_2C_2H_2)_2(S_2C_2H_4)_2$.[31]

We propose that **10** forms via the intermediacy of $\{ReS[S_2C_2(tms)_2](SH)(SC_2H_4SH)\}^-$, which cyclizes with elimination of H_2S. This proposed pathway was supported by studies using 2-mercaptoethanol. A solution of **1**, HOC_2H_4SH, and diphenylacetylene afforded an isolable adduct whose ^1H NMR, ^{13}C NMR, and mass spectral data are consistent with its description as $[ReS(S_2C_2Ph_2)(SH)(SC_2H_4OH)]^-$ (**11**). This adduct shows no evidence of elimination of H_2S (or H_2O) (eq 4). In an

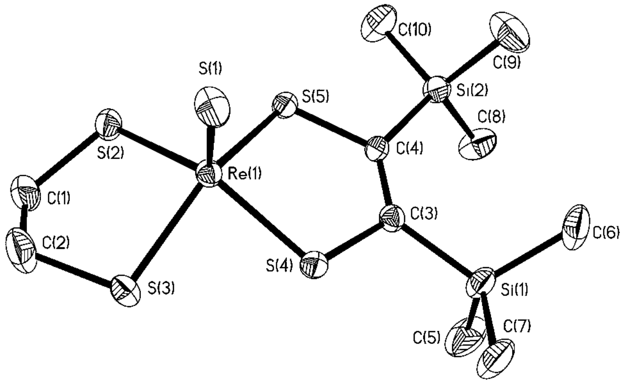

Figure 3. Structure of the anion $\{ReS[S_2C_2(tms)_2](S_2C_2H_4)\}^-$ (**10**) with thermal ellipsoids drawn at the 35% probability level. Hydrogen atoms are omitted for clarity.

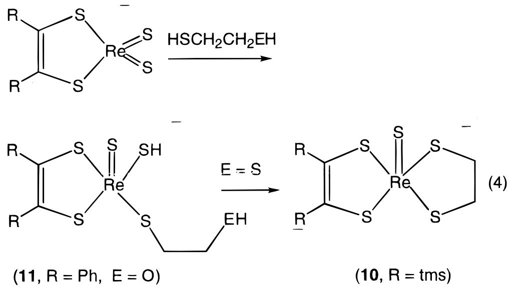

(4)

interesting extension of this methodology, treatment of a C_2H_4-purged solution of **1** with $C_2H_4(SH)_2$ yields $[ReS(S_2C_2H_4)_2]^-$ (**12**) together with H_2S (eq 5).

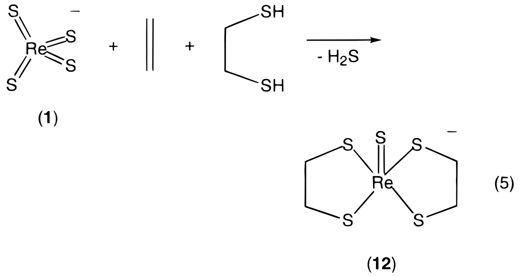

(5)

In principle, a range of unsymmetrical bis(chelate) derivatives of Re^V could be prepared by the alkene/dithiol reaction. An attempted reaction of 1,3-propanedithiol, **1**, and C_2H_4 failed to produce $[ReS(S_2C_2H_4)(S_2C_3H_6)]^-$. The ^1H NMR spectrum of the product mixture exhibited several MS*H* signals and a large number of resonances in the methylene region. Some **1** was still observed in the reaction mixture after extended reaction periods. Thus 1,3-propanedithiol is less effective than ethanedithiol in binding $[ReS_2(S_2C_2H_4)]^-$. Similarly, the reaction of **1**, C_2H_4, and $CH_2{=}CHCH_2SH$ failed to pro-

---

(31) Tisato, F.; Bolzati, C.; Duatti, A.; Bandoli, G.; Refosco, F. *Inorg. Chem.* **1993**, *32*, 2042−2048. It has been recently suggested that Tisato et al.'s $Tc_2(S_2C_2H_2)_2(S_2C_2H_4)_2$ should be formulated $Tc_2(S_2C_2H_4)_4$. See: Lente, G.; Shan, X.; Guzei, I. A.; Espenson, J. H. *Inorg. Chem.* **2000**, *39*, 3572−3576.

Scheme 4

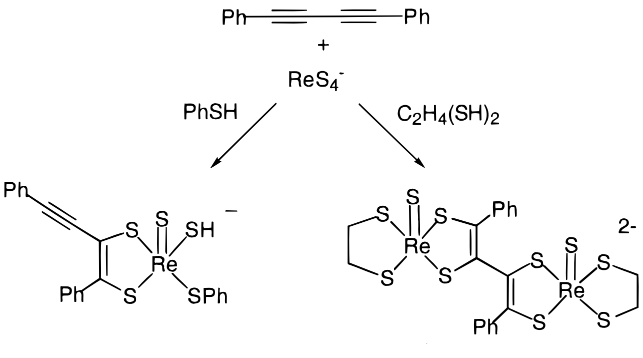

(**13**, one of two isomers) (**14**, one of two isomers)

duce a stable derivative. Apparently, the cyclization to form 1,3-propanedithiolato derivatives of Re(V) species is significantly less favored than the formation of the more stable 1,2-dithiolates.

Reactions Involving Diynes. Dithiolenes derived from diynes have not been investigated, although such reactions could give rise to interesting binuclear bis(dithiolene) complexes.[32,33] The reaction of **1**, PhSH, and 1,4-diphenylbutadiyne afforded the alkynyl-substituted dithiolene $\{ReS[S_2C_2Ph(C_2Ph)](SH)(SPh)\}^-$ (**13**), which was identified by elemental analysis, ^1H NMR spectroscopy, and ESI-MS. Two isomers were observed in ca. 1:1 ratio based on the intensities of $-SH$ resonances (δ 6.29, 6.36) in the ^1H NMR spectrum. Attempts to prepare a bismetalated diyne led to only low yields, even in the presence of excess **1** and PhSH.

The analogous reaction of **1**, Ph_2C_4, and $C_2H_4(SH)_2$ provided the desired bismetalated species $(Ph_4P)_2\{[ReS(S_2C_2H_4)]_2(S_4C_4Ph_2)\}$ (**14**) (Scheme 4). Loss of H_2S drives the formation of the bismetalated product. UV−visible spectroscopic measurements show that 1 equiv of **1** is rapidly consumed, while the addition of a second equiv of **1** requires hours. Compound **14** was identified by mass spectrometry and elemental analyses. Its ^1H NMR spectrum is consistent with the presence of isomers, as both the methylene and the phenyl signals are significantly broadened. Isomerism arises from the two orientations of the Re═S functionalities relative to the C_4S_4 plane defined by the 1,2,3,4-butadienetetrathiolate.

Summary and Conclusions

In this work, we have shown that H_2S and organic thiols strongly influence the binding of unsaturated substrates to tetrathiorhenate centers. In contrast to ReS_4^-, the d^2 tetrahedral adducts $ReS_2(S_2un)^-$ (un = alkene or alkyne) readily bind RSH reagents. The reactivity is particularly striking in the case of alkenes that interact only feebly with **1**. In the presence of H_2S or thiols, however, one can readily observe the adducts $ReS(S_2C_2H_3R)(SH)(SR')^-$. The energetics of the relevant reactions are illustrated qualitatively in Scheme 5.

Scheme 5. Qualitative Reaction Coordinate, Illustrating the Coupling of RSH and Alkene Additions to ReS_4^-.

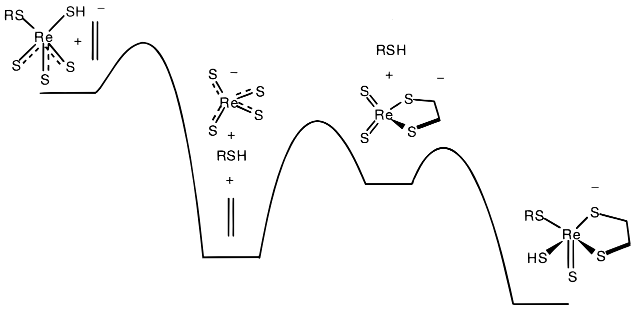

Tetrahedral M(═E)(═E′)X_2 complexes are known to bind reagents to give d^2 square pyramidal derivatives. Quantum chemical calculations by Rappé and Goddard show that such reactions are driven by the formation of one strongly bonded terminal M═E (E = O, NR) unit.[34] This “spectator oxo effect” has been invoked to explain the binding of alkenes to the alkylidene complexes $(RO)_2Mo(NR)(CR_2)$. Coucouvanis has proposed an analogous spectator sulfido effect to explain the reactivity of tetrahedral $Mo({=}S)_2X_2$ species.[13] In the present case, the very stabilizing $X_4Re^V{=}S$ species arises by the addition of RSH across a Re═S bond.

The addition of thiols to $[ReS_2(S_2C_2R_n)]^-$ represents an unusual route to SH-containing dithiolene complexes, a class of compounds previously proposed to exist in the catalytic cycle of xanthine oxidase.[26−29] The addition of H_2S across d^0 Re═O bonds was recently considered in the context of the CH_3ReO_3-catalyzed desulfurization of thiiranes (eq 6).[35] Sulfido metallocenes add H_2S to give adducts of the form $Cp^*_2M(SH)_2$ (M = Ti, Mo).[9,36]

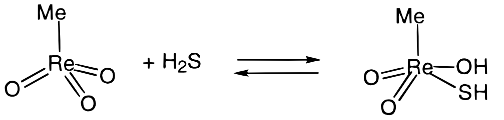

$$\mathrm{MeRe({=}O)_3} + \mathrm{H_2S} \rightleftharpoons \mathrm{MeRe({=}O)_2(OH)(SH)} \qquad (6)$$

In contrast to monthiols, ethanedithiol adds irreversibly to $Re^V{=}S$ bonds due to the loss of H_2S. The addition of ethanedithiol is analogous to the formation of 1,3-dithiolanes from ketones and ethanedithiol. The irreversibility of this H_2S elimination step allows one to force otherwise unfavorable equilibria as illustrated by the synthesis of $[ReS(S_2C_2H_4)_2]^-$ from ReS_4^-, ethanedithiol, and ethylene and by the preparation of the butadienetetrathiolate $\{[ReS(S_2C_2H_4)]_2(S_4C_4Ph_2)\}^-$ from ReS_4^-, ethanedithiol, and 1,4-diphenylbutadiyne.

Experimental Section

Reactions were conducted with standard inert-atmosphere techniques unless otherwise stated. Procedures for the purification of reagents and solvents have been recently described.[15] ^1H (400 MHz) and ^{13}C (100 MHz) NMR spectra were acquired on a Varian Unity 400 spectrometer using residual solvent ^1H and ^{13}C resonances as internal references. Electrospray ionization mass spectra were acquired using freshly prepared CH_3CN solutions. Masses are reported for the most abundant peak in the mass envelopes. The solubilities of H_2S in various reaction solvents have been quantified.[37] D_2S was generated by the addition of D_2O to solid P_4S_{10}.

$Ph_4P\{ReS[S_2C_2(tms)_2](SH)_2\}$, Ph_4P[2]. A 100 mL Schlenk flask was charged with 0.117 g (0.177 mmol) of Ph_4P[**1**]. The solid was slurried in 5 mL of CH_3CN, and a light purge of H_2S was established through the vessel. A solution of 0.17 g (1.02 mmol) of $C_2(tms)_2$ in 5 mL of CH_3CN was added to the stirred slurry dropwise by syringe over ca. 5 min. The undissolved Ph_4P[**1**] was drawn into solution as

---

(32) Kajitani, M.; Hagino, G.; Tamada, M.; Fukita, T.; Sakurada, M.; Akiyama, T.; Sugimori, A. *J. Am. Chem. Soc.* **1996**, *118*, 489−490.

(33) Keefer, C. E.; Purrington, S. T.; Bereman, R. D.; Boyle, P. D. *Inorg. Chem.* **1999**, *38*, 5437−5442.

(34) Rappé, A. K.; Goddard, W. A., III. *J. Am. Chem. Soc.* **1982**, *104*, 3287−3294.

(35) Jacob, J.; Espenson, J. H. *Chem. Commun.* **1999**, 1003−1004.

(36) Pilato, R. S.; Eriksen, K. A.; Stiefel, E. I.; Rheingold, A. L. *Inorg. Chem.* **1993**, *32*, 3799−3800.

(37) Fogg, P. G. T., Young, C. L., Eds. *Hydrogen Sulfide, Deuterium Sulfide, and Hydrogen Selenide*; Pergamon Press: Oxford, U.K., 1988.

the flask contents turned red-brown. When the addition was complete, the flask was closed under an atmosphere of H_2S, and the mixture was stirred for an additional 15 min, after which 150 mL of 1:1 Et_2O/hexanes was added and the contents were cooled in an ice bath. Excess H_2S was removed by evacuating the cooled vessel until a tacky precipitate formed and the solution became almost colorless. The solution was decanted from the red-brown residue, which was triturated twice with 50 mL portions of hexanes. Yield: 0.130 g (79%). A CD_3CN solution of **3** converted to *cis*- and *trans*-$\{ReS(\mu\text{-}S)[C_2S_2(tms)_2]\}_2^{2-}$ (~80%) after 24 h. Attempts to isolate the product by stripping the CH_3CN away from the crude reaction mixture *in vacuo* resulted in contamination by significant quantities of *cis*- and *trans*-$\{ReS(\mu\text{-}S)[C_2S_2(tms)_2]\}_2^{2-}$.[17] Anal. Calcd (found): C, 44.78 (44.85); H, 4.70 (4.66). ^1H NMR (CD_3CN): δ 5.98 (s, 2H, S*H*), 0.46 (s, 18H, Si*Me*$_3$). ^{13}C NMR (CD_3CN): δ 165.9 (2C), 2.12 (6C). ESI-MS: *m*/*z* 519.1 (M^-).

$Ph_4P[ReS(S_2C_7H_{10})(SH)_2]$, Ph_4P[3]. A slurry of 0.160 g (0.245 mmol) of Ph_4P[**1**] in 10 mL of CH_3CN was treated with a solution of 0.043 g (0.457 mmol) of norbornene in 5 mL of CH_3CN, resulting in a color change to yellow and the appearance of a gold-colored precipitate. The vessel was then purged with H_2S and sealed. Over the course of 1 h, the gold precipitate converted to a brown solid. The reaction mixture was treated with 60 mL of 1:1 hexane/Et_2O to complete the precipitation. After removal of the supernatant with a cannula, the brown solids were dissolved in ~10 mL of CH_3CN and reprecipitated by the addition of 75 mL of Et_2O. Yield: 0.17 g (88%) of a mixture of isomers A and B (a single isomer (isomer A) was obtained if the pot mixture was stirred for ca. 16 h under an atmosphere of H_2S). A Sample of the 1:1 isomer mixture was sealed in an NMR tube under vacuum and monitored for several days. ^1H NMR studies showed that, over the course of 96 h, both isomers decomposed at similar rates to the adduct $[ReS_2(S_2C_7H_{10})]^-$. Anal. Calcd (found): C, 47.61 (47.23); H, 4.12 (4.10). ^1H NMR (CD_3CN): isomer A δ 6.07 (s, 1H), 3.24 (d, $J = 1.8$ Hz, 2H), 2.53 (m, 2H), 1.60 (m, 2H), 1.40 (m, 2H), 1.15 (dm, $J = 9.6$ and 1.9 Hz, 1H), 1.02 (dm, $J = 9.6$ and 1.6 Hz, 1H); isomer B δ 6.08 (s, 1H), 3.53 (d, $J = 1.7$ Hz, 2H), 2.42 (m, 2H), 1.53 (m, 2H), 1.33 (m, 3H), 0.94 (dm, $J = 9.6$ and 1.6 Hz, 1H). ESI-MS: *m*/*z* 442.9 (M^-).

Deuterium Exchange of Ph_4P[3]. Dideuterated **3** (**3**-*d*$_2$) was generated in a manner analogous to that for **3** using D_2S in place of H_2S. ^1H NMR spectroscopy showed all of the resonances associated with the norbornyl backbone of **3**, but the intensities of the −S*H* resonances were only ca. 2% of the theoretical values. A 5 mm NMR tube was charged with 5.2 mg (0.006 mmol) of Ph_4P[**3**-*d*$_2$], 0.89 mL of CD_3CN, and ~1 atm of H_2S (a 10-fold excess indicated by subsequent ^1H NMR integration). The ^1H NMR spectrum was then monitored using the Ph_4P^+ cation as an internal integration standard. The intensities of the Re−S*H* signals due to **3** had ceased to increase after 57 h (66% of the theoretical maxima). No significant change in the isomer distribution of **3** was observed over the duration of the experiment.

$Ph_4P[ReS(S_2C_2H_4)(SH)_2]$, Ph_4P[4]. A 5 mm NMR tube was charged with 3.5 mg (0.005 mmol) of Ph_4P[**1**], ~1 mL of CD_3CN, and excess H_2S and C_2H_4. The ^1H NMR spectrum indicated ~60% conversion to $[ReS(S_2C_2H_4)(SH)_2]^-$ based on the integration of Ph_4P^+ resonances vs those of bound ethylene. ^1H NMR: δ 3.05 (AA′BB′, 2H), 6.54 (s, 2H). A sample of Ph_4P[**4**] generated by condensation of H_2S and C_2H_4 onto a CH_3CN solution of Ph_4P[**1**] in a 100 mL flask was evacuated to remove all volatile components. The solution became red-violet prior to yielding a red-violet solid, which was recrystallized from CH_3CN/Et_2O and dried *in vacuo*. The microcrystalline violet product was identified as Ph_4P[**1**] by UV−visible spectroscopy.[38]

$Ph_4P[ReS(S_2C_7H_{10})(SH)(SeH)]$, Ph_4P[5]. A 5 mm NMR tube was charged with ~5 mg (ca. 0.006 mmol) of $Ph_4P[ReS_2(S_2C_7H_{10})]$, ~1 mL of CD_3CN, and ~3 equiv excess of H_2Se and flame-sealed under dynamic vacuum. The ^1H NMR spectrum, recorded immediately upon warming the mixture to ambient temperature, indicated complete conversion to $[ReS(S_2C_7H_{10})(SH)(SeH)]^-$ and the absence of $[ReS_2(S_2C_7H_{10})]^-$. After 20 min (room temperature), decomposition was evident. After 3 h, signals due to **5** were barely detectable. ^1H NMR: δ 6.71 (s, 1H, $^3J_{SeH} = 13.5$ Hz), 6.67 (s, 1H, $^3J_{SeH} = 13.5$ Hz), 3.52 (dd, 1H, $J = 7.96$ and 1.75 Hz), 3.39 (dd, 1H, $J = 7.96$ and 1.75 Hz), 3.24 (dd, 1H, $J = 8.70$ and 1.72 Hz), 3.18 (dd, 1H, $J = 8.70$ and 1.72 Hz), 2.56 (m, 1H), 2.54 (m, 1H), 2.51 (s, 1H), 2.49 (s, 1H), 2.44 (m, 1H), 2.42 (m, 1H), 1.58−1.62 (m, 2H), 1.51−1.56 (m, 2H), 1.37−1.42 (m, 2H), 1.31−1.36 (m, 3H), 1.12 (dm, 1H, $J = 9.30$ and 2.01 Hz), 1.01 (dm, 1H, $J = 9.60$ and 1.67 Hz), 0.93 (dm, 1H, $J = 9.65$ and 1.67 Hz).

Table 2. Selected Bond Distances (Å) for **8**

Re(1)−S(1)	2.107(3)	Re(1)−S(2)	2.290(3)
Re(1)−S(3)	2.279(3)	Re(1)−S(4)	2.338(3)
Re(1)−S(5)	2.352(3)	S(2)−C(8)	1.824(15)
S(4)−C(1)	1.785(12)	S(3)−C(7)	1.93(5)
C(1)−C(6)	1.389(18)	C(1)−C(2)	1.374(18)
C(3)−C(4)	1.36(2)	C(2)−C(3)	1.41(2)
C(5)−C(6)	1.363(17)	C(4)−C(5)	1.40(2)
C(7)−C(8)	1.49(6)		

$Ph_4P\{ReS[S_2C_2(tms)_2](SH)(SPh)\}$, Ph_4P[6]. A slurry of 0.260 g (0.398 mmol) of Ph_4P[**1**] in 10 mL of CH_3CN in a 200 mL Schlenk flask was treated with 0.05 mL (0.52 mmol) of benzenethiol. A solution of 0.38 g (2.23 mmol) of $C_2(tms)_2$ in 5 mL of CH_3CN was added dropwise over 10 min, causing an immediate color change from violet to dark red-brown. After 1 h, the flask contents were condensed *in vacuo* to ~5 mL and treated with 100 mL of 1:1 Et_2O/hexanes to produce a red-brown oil. The residue was extracted into 3 mL of CH_3CN, and the red-brown product was precipitated by addition of 100 mL of 1:1 Et_2O/hexanes. Yield: 0.34 g (91%). Anal. Calcd (found): C, 48.84 (48.57); H, 4.74 (4.71); S, 17.15 (17.35); Si, 6.01 (6.19); P, 3.31 (3.18). ^1H NMR (CD_3CN): δ 7.82 (m, 2H), 7.35 (m, 2H), 7.19 (m, 1H), 5.82 (s, 1H), 0.43 (s, 9H), 0.27 (s, 9H). ^{13}C NMR (CD_3CN): δ 167.5 (1C), 166.9 (1C), 135.3 (1C), 135.1 (2C), 128.9 (2C), 126.2 (1C), 7.8 (6C). ESI-MS: *m*/*z* 595.2 (M^-).

$Ph_4P[ReS(S_2C_7H_{10})(SH)(SPh)]$, Ph_4P[7]. A slurry of 0.210 g (0.321 mmol) of Ph_4P[**1**] in 15 mL of CH_3CN was treated with a solution of 0.048 g (0.511 mmol) of norbornene in 5 mL of CH_3CN. The solution immediately turned yellow, and precipitation of golden $Ph_4P[ReS_2(S_2C_7H_{10})]$ was observed. The reaction mixture was then treated with 0.05 mL (0.52 mmol) of benzenethiol. Over the course of 2 h, the precipitate dissolved to give a red-brown solution. The flask contents were concentrated to ~5 mL under vacuum and treated with 50 mL of Et_2O to deposit a brown precipitate. The crude product was extracted into a minimum amount (~10 mL) of CH_3CN and reprecipitated with 75 mL of Et_2O. Yield: 0.25 g (0.29 mmol, 90%). Two isomers were noted on the basis of two different −S*H* resonances in the ^1H NMR spectrum. Anal. Calcd (found): C, 51.78 (50.76); H, 4.23 (4.14); S, 18.68 (18.34); P, 3.61 (3.53). ^1H NMR (CD_3CN): δ 7.78 (m, 4H), 7.30 (m, 4H), 7.14 (m, 2H), 5.91 (s, −SH), 5.87 (s, −SH), 3.23 (d, $J = 1.7$ Hz, 1H), 3.20 (d, $J = 1.7$ Hz, 1H), 3.10 (d, $J = 1.7$ Hz, 1H), 3.08 (d, $J = 1.7$, 1H), 2.53 (m, 1H), 2.39 (m, 1H), 2.32 (m, 1H), 2.27 (m, 1H), 1.45−1.61 (m, 4H), 1.24−1.40 (m, 4H), 1.06 (dm, $J = 9.5$ and 1.8 Hz, 1H), 0.89−0.97 (m, 3H). ESI-MS: *m*/*z* 519.1 (M^-).

$Ph_4P[ReS(S_2C_2H_4)(SH)(SPh)]$, Ph_4P[8]. A slurry of 0.167 g (0.256 mmol) of Ph_4P[**1**] in 15 mL of CH_3CN was treated with 0.03 mL (0.29 mmol) of benzenethiol, and the mixture was purged lightly with ethylene for 30 min, during which the solution turned dark red. The vessel was then closed, and the contents were stirred under an atmosphere of ethylene. After 1 h, the solution was concentrated to ~5 mL under vacuum, and the concentrate was treated with 50 mL of Et_2O to deposit a dark brown precipitate. The precipitate was dissolved in 10 mL of CH_3CN, after which the solution was concentrated to ~5 mL *in vacuo* and diluted with 60 mL of Et_2O to give brown microcrystals. Yield: 0.18 g (89%). Anal. Calcd (found): C, 48.52 (47.85); H, 3.82 (3.81); P, 3.91 (3.58); S, 20.24 (20.30). ^1H NMR (CD_3CN): δ 2.75 (m, 2H), 3.03 (m, 1H), 3.21 (m, 1H), 6.45 (s, SH), 7.12−7.17 (m, 1H), 7.29−7.34 (m, 2H), 7.75−7.79 (m, 2H). ESI-MS: *m*/*z* 453.1 (M^-).

$Ph_4P[ReS(S_2C_6H_{12})(SH)(SPh)]$, Ph_4P[9]. A solution of 2.0 mg (0.003 mmol) of Ph_4P[**1**], 1-hexene, PhSH, and 0.86 g of CD_3CN was flame-sealed in a 5 mm NMR tube. Over the course of 12 h, the violet

---

[38] Do, Y.; Simhon, E. D.; Holm, R. H. *Inorg. Chem.* **1985**, *24*, 4635−4642.

Table 3. Selected Bond Angles (deg) for **8**

S(1)−Re(1)−S(3)	109.85(13)	S(1)−Re(1)−S(2)	108.25(13)
S(2)−Re(1)−S(3)	84.89(12)	S(1)−Re(1)−S(4)	108.29(12)
S(3)−Re(1)−S(4)	86.88(11)	S(2)−Re(1)−S(4)	143.20(11)
S(1)−Re(1)−S(5)	109.06(11)	S(3)−Re(1)−S(5)	141.07(13)
S(2)−Re(1)−S(5)	82.03(12)	S(4)−Re(1)−S(5)	82.19(11)
C(8)−S(2)−Re(1)	105.9(5)	C(7)−C(8)−S(2)	122.2(2)
C(8)−C(7)−S(3)	106(4)	C(7)−S(3)−Re(1)	106.7(13)
C(1)−S(4)−Re(1)	113.7(4)	C(2)−C(1)−C(6)	118.3(12)
C(2)−C(1)−S(4)	118.4(11)	C(6)−C(1)−S(4)	123.1(10)
C(1)−C(2)−C(3)	121.7(14)	C(4)−C(3)−C(2)	118.6(14)
C(3)−C(4)−C(5)	120.2(14)	C(6)−C(5)−C(4)	120.7(14)
C(5)−C(6)−C(1)	120.6(13)		

Table 4. Selected Bond Distances (Å) for **10**

Re(1)−S(1)	2.1084(11)	Re(1)−S(4)	2.2922(10)
Re(1)−S(5)	2.2994(10)	Re(1)−S(2)	2.3157(10)
Re(1)−S(3)	2.3202(10)	S(2)−C(1)	1.821(5)
S(3)−C(2)	1.846(5)	S(4)−C(3)	1.787(4)
S(5)−C(4)	1.771(4)	Si(1)−C(5)	1.861(5)
Si(1)−C(6)	1.874(5)	Si(1)−C(7)	1.879(5)
Si(1)−C(3)	1.883(4)	Si(2)−C(9)	1.844(5)
Si(2)−C(10)	1.858(4)	Si(2)−C(8)	1.869(4)
Si(2)−C(4)	1.889(4)	C(1)−C(2)	1.452(6)
C(3)−C(4)	1.348(5)		

Table 5. Selected Bond Angles (deg) for **10**

S(1)−Re(1)−S(4)	109.54(4)	S(1)−Re(1)−S(5)	108.31(4)
S(4)−Re(1)−S(5)	82.49(3)	S(1)−Re(1)−S(2)	110.72(4)
S(4)−Re(1)−S(2)	139.66(4)	S(5)−Re(1)−S(2)	82.72(4)
S(1)−Re(1)−S(3)	109.09(4)	S(4)−Re(1)−S(3)	84.73(4)
S(5)−Re(1)−S(3)	142.59(4)	S(2)−Re(1)−S(3)	84.70(4)
C(1)−S(2)−Re(1)	108.43(15)	C(2)−S(3)−Re(1)	103.90(17)
C(3)−S(4)−Re(1)	109.82(12)	C(4)−S(5)−Re(1)	109.76(12)
C(5)−Si(1)−C(6)	111.1(3)	C(5)−Si(1)−C(7)	109.1(3)
C(6)−Si(1)−C(7)	103.6(2)	C(5)−Si(1)−C(3)	108.9(2)
C(6)−Si(1)−C(3)	114.0(2)	C(7)−Si(1)−C(3)	110.09(19)
C(2)−C(1)−S(2)	113.5(4)	C(1)−C(2)−S(3)	112.6(4)
C(4)−C(3)−S(4)	117.8(3)	C(4)−C(3)−Si(1)	129.6(3)
S(4)−C(3)−Si(1)	112.53(19)	C(3)−C(4)−S(5)	118.6(3)
C(3)−C(4)−Si(2)	130.2(3)	S(5)−C(4)−Si(2)	111.26(18)

Table 6. Crystallographic Data and Structure Solution Details for Ph_4P[**8**] and Ph_4P[**10**]·$0.5CH_3CN$

empirical formula	$C_{32}H_{30}PReS_5$	$C_{35}H_{42}PReS_5Si_20.5CH_3CN$
fw	791.02	904.85
crystal system	triclinic	monoclinic
space group	$P\bar{1}$ (No. 2)	$P2_1/c$ (No. 14)
a (Å)	10.917(2)	10.8920(6)
b (Å)	11.588(2)	15.0195(8)
c (Å)	13.859(3)	24.8296(14)
α (deg)	85.742(3)	90
β (deg)	89.972(3)	99.3340(10)
γ (deg)	63.378(3)	90
V (Å^3)	1562.1(5)	4008.2(4)
Z	2	4
ρ_{calcd} (Mg/m^3)	1.682	1.499
ab coeff (mm^{-1})	4.296	3.416
F_{000}	782	1820
θ range (deg)	1.47−28.26	1.59−28.34
reflns collected/unique	9932/7060	24714/9487
data/restraints/params	7060/0/362	9487/3/419
R(int)	0.0778	0.0506
goodness-of-fit on F^2	0.944	1.052
final R indices [$I > 2\sigma(I)$]: R1, wR2	0.0735, 0.1768	0.0338, 0.0773
R indices (all data): R1, wR2	0.1196, 0.1992	0.0605, 0.0849

color of **1** changed to brown-yellow. The ^1H NMR spectrum of the tube contents showed ∼68% conversion to **9** at room temperature with a relative ratio of **1**:hexene:PhSH = ca. 1:21:29 ($K_{eq} = 402\ M^{-2}$). The product was identified on the basis of the four terminal Re−S*H* signals located at δ 6.54, 6.43, 6.39, and 6.38. Resonances for the C_4H_9 portion of the 1,2-hexanedithiolate ligand (δ 2.20−3.30) were not analyzed.

Thermodynamic data were obtained from ^1H NMR spectra recorded at 50, 40, 30, 21, 0, and −20 °C (Table 1). At each temperature, the concentration of the contributing species was assayed by integration (against Ph_4P^+) of the signals at δ 5.85 ($H_2C{=}CH(C_4H_9)$) and 3.88 (PhS*H*). The concentration of the product, **9**, was measured as the sum of the four Re−S*H* signals generated by the four observed isomers. The concentration of **1** was assumed to be $(I_{Ph_4P}/4) - \sum I_{ReSH}$, where I_X is the integrated intensity of the signal for species X and the integration of Ph_4P^+ utilized the proton resonance due to the hydrogens in the para positions relative to phosphorus. To ensure reliable integrations, we employed a 40 s delay between pulses. The temperature was calibrated by the chemical shifts of neat methanol.

Ph_4P{ReS[S_2C_2(tms)$_2$]($S_2C_2H_4$)}, Ph_4P[10]. A slurry of 0.159 g (0.243 mmol) of Ph_4P[**1**] in 5 mL of CH_3CN and 0.05 mL (0.60 mmol) of ethanedithiol was treated with a solution of 0.17 g (0.99 mmol) of C_2(tms)$_2$ in 5 mL of CH_3CN, which was added dropwise over 5 min. The reaction mixture rapidly turned brown-red and was then briefly purged with N_2. A test of the effluent purge gas with moist Pb(O_2CCH_3)$_2$-impregnated paper indicated H_2S. After 2 h, the solvent volume was reduced to ∼5 mL, and the concentrate was treated with 60 mL of 1:1 hexane/Et_2O to give an oily red-brown residue. The oily residue was crystallized by dissolution in 3 mL of CH_3CN followed by addition of 80 mL of 1:1 hexane/Et_2O. Yield: 0.19 g (88%). Anal. Calcd (found): C, 46.18 (45.84); H, 4.79 (4.97); P, 3.50 (3.34); S, 18.12 (18.37); Si, 6.35 (6.38). ^1H NMR (CD_3CN): δ 2.71 (m, AA′BB′, 4H), 0.42 (s, 18H). ^{13}C NMR (CD_3CN): δ 163.2 (2C), 45.2 (2C), 3.3 (6C). ESI-MS: *m*/*z* 545.2 (M^-).

Ph_4P[ReS($S_2C_2Ph_2$)(SCH_2CH_2OH)(SH)], Ph_4P[11]. A 100 mL Schlenk flask was charged with 0.131 g (0.200 mmol) of Ph_4P[**1**], 10 mL of CH_3CN, and 0.05 mL (0.713 mmol) of 2-mercaptoethanol. A solution of 0.095 g (0.540 mmol) of diphenylacetylene in 10 mL of CH_3CN was added to the slurry dropwise over 30 min. After 3 h, the resulting red-brown solution was concentrated to ∼5 mL under vacuum. A dark red, oily precipitate formed upon addition of 60 mL of 1:1 Et_2O/hexanes. The residue was dissolved in 10 mL of CH_3CN, the solution was condensed to ca. 5 mL, and the red-brown product was precipitated with 75 mL of Et_2O. Yield: 0.170 g (93%). Anal. Calcd (found): C, 52.78 (52.89); H, 3.99 (3.74); S, 17.61 (17.46); P, 3.40 (3.01). ^1H NMR (CD_3CN): δ 7.18−7.29 (m, 10H), 6.07 (s, 1H), 3.97 (br m, 2H), 3.81 (m, 2H), 2.76 (br t, 1H). ^{13}C NMR (CD_3CN): δ 141.4 (1C), 140.9 (1C), 130.1 (2C), 130.0 (2C), 127.8 (2C), 127.7 (2C), 127.6 (1C), 127.5 (1C), 126.9 (1C), 126.8 (1C), 63.7 (1C), 41.9 (1C). ESI-MS: *m*/*z* 571.2 (M^-).

Ph_4P[SRe($S_2C_2H_4$)$_2$], Ph_4P[12], from Ph_4P[1], C_2H_4, and C_2H_4(SH)$_2$. A light purge of ethylene was established over a slurry of 0.150 g (0.229 mmol) of Ph_4P[**1**] in 10 mL of CH_3CN and 0.05 mL (0.60 mmol) of ethanedithiol. Over the course of 30 min, brick red microcrystals appeared. A test of the effluent purge gas with moist Pb(O_2CCH_3)$_2$-impregnated paper indicated H_2S. The purge was discontinued after 1 h, and the flask contents were stirred under an atmosphere of ethylene for an additional 1 h. The slurry was concentrated to ca. 5 mL under vacuum, and the product was precipitated by the addition of 50 mL of Et_2O. The microcrystalline solid was recrystallized twice from CH_3CN/Et_2O. Yield: 0.15 g (88%). Anal. Calcd (found): C, 45.32 (45.20); H, 3.80 (3.88). ESI-MS: *m*/*z* 403.1 (M^-). The product was identified by comparison of its ^1H NMR data to literature values.[39]

Ph_4P{ReS[S_2C_2Ph(C_2Ph)](SH)(SPh)}, Ph_4P[13]. A solution of 0.118 g (0.181 mmol) of Ph_4P[**1**] in 130 mL of CH_3CN was added dropwise to a solution of 0.300 g (1.48 mmol) of diphenylbutadiyne and 0.20 mL (2.08 mmol) of benzenethiol in 20 mL of CH_3CN. The mixture turned brown over the course of the addition of **1**. After 2 h, the volatile components were removed under vacuum, and the glassy residue was extracted into 5 mL of CH_3CN. Addition of 100 mL of 1:1 Et_2O/hexanes produced a brown precipitate. The extraction/precipitation procedure was repeated three times to give the pure brown

---

(39) Blower, P. J.; Dilworth, J. R.; Hutchinson, J. P.; Zubieta, J. A. *Inorg. Chim. Acta* **1982**, *65*, L225−L226.

solid product. Yield: 0.112 g (64%). Anal. Calcd (found): C, 57.17 (57.05); H, 3.75 (3.48); S, 16.58 (16.80). ^{1}H NMR (CD_3CN): δ 6.29 (s, 1H), 6.36 (s, 1H), 7.20−7.48 (m, 24H), 7.65 (dm, $J = 7.7$ Hz, 2H), 7.84−7.90 (m, 4H). ESI-MS: 627.1 (M^-).

$(Ph_4P)_2\{[ReS(S_2C_2H_4)]_2(S_4C_4Ph_2)\}$ 14. A solution of 0.220 g (0.336 mmol) of Ph_4P[**1**], 30 mL of CH_3CN, and 0.50 mL (6.0 mmol) of ethanedithiol was treated with a solution of 33 mg (0.168 mmol) of 1,4-diphenylbutadiyne in 30 mL of CH_3CN, which was added dropwise over the course of 1 h. The resulting red-brown solution was stirred for an additional 8 h, after which UV−visible analysis indicated the complete consumption of **1**. The solution was concentrated to ∼10 mL *in vacuo*, and a brown precipitate formed upon addition of 60 mL of Et_2O. The crude product was extracted into 10 mL of CH_3CN and precipitated as a brown solid by the addition of the CH_3CN solution to a flask containing 75 mL of Et_2O. Yield: 0.26 g (94%). Anal. Calcd (found): C, 50.10 (49.31); H, 3.58 (3.52); S, 19.66 (19.82); P, 3.80 (3.85). ^{1}H NMR (CD_3CN): δ 2.76 (br, 4H), 2.84 (br, 4H), 6.81−7.15 (br, 6H), 7.23−7.38 (br, 4H). ESI-MS: *m*/*z* 1289.4 (Ph_4P[**14**]$^-$), 474.8 ([**14**]$^{2-}$).

Crystallographic Characterization of Ph_4P[8] and Ph_4P[10]. Single crystals of Ph_4P[**8**] were obtained as red prisms by careful layering of a CH_3CN solution with Et_2O. A crystal was chosen and mounted on a glass fiber with Paratone-E (Exxon). The space group $P\bar{1}$ (No. 2) was selected on the basis of systematic conditions and was verified by subsequent refinement. The structure was solved by direct methods and refined by full-matrix least-squares calculations based on F^2. Hydrogen atom positions were calculated using a riding model, and non-hydrogen atoms were refined anisotropically. A disorder in the ethanedithiolate backbone (C(7), C(7B)) was modeled on the basis of occupancy factors of 32.2 and 77.8%. Tabular data reflect the more highly populated C(7) position. The largest peak and hole in the difference map were determined to be 3.690 and −4.841 e·Å^{-3}, respectively. Relevant metrical and crystallographic data are collected in Tables 2, 3, and 6.

Single crystals of Ph_4P[**10**]·$0.5CH_3CN$ were obtained as red prisms by careful layering of a CH_3CN solution with Et_2O. A crystal was chosen and mounted on a glass fiber with Paratone-E (Exxon). The space group $P2_1/c$ (No. 14) was selected on the basis of systematic conditions and was verified by subsequent refinement. The structure was solved by direct methods and refined by full-matrix least-squares calculations based on F^2. Hydrogen atom positions were calculated using a riding model. Non-hydrogen atoms were refined anisotropically, with the exception of those of the acetonitrile solvent molecule, which was refined as a rigid unit and determined to be disordered over two positions surrounding the inversion center. The largest peak and hole in the difference map were determined to be 1.210 and −1.215 e·Å^{-3}, respectively. Relevant metrical and crystallographic data are collected in Tables 4−6.

Acknowledgment. This research was supported by the U.S. Department of Energy and the National Science Foundation. We thank J. G. Breitzer for assistance with the thermodynamic measurements.

Supporting Information Available: Listings of X-ray experimental details, atomic coordinates, thermal parameters, bond distances, and bond angles for Ph_4P[**8**] and Ph_4P[**10**]. This material is available free of charge via the Internet at http://pubs.acs.org.

IC0001661